Quantum Connected Collaborative Learning with Superdense Coding for Wireless Internet-of-Everything Networks

(Invited Paper)

Goki F. R. Purba*, Bhaskara Narottama*, Saeed R. Khosravirad†, Simon L. Cotton‡, Trung Q. Duong*‡,
*Memorial University, Canada
†Nokia Bell Labs, USA
‡Queen's University Belfast, Belfast, U.K
e-mail: {gfrpurba, bnarottama}@mun.ca, saeed.khosravirad@nokia-bell-labs.com, simon.cotton@qub.ac.uk, tduong@mun.ca

***Abstract*—In recent years, distributed wireless communication optimization, where training data is stored remotely from local multi-access edge computing (MEC) processors to preserve data security privacy and minimize complexity, has seen noteworthy progress for relevant wireless Internet-of-Everything (WIoE) networks beyond 6G. Nonetheless, the exploding number of WIoE clients requires secure data storage and scaled data processing at the network and transmitter, which local processors might be unable to afford. Parallel to this, we are witnessing widespread quantum-enabled learning adoptions for optimizing wireless communications. The rapid growth of quantum technologies has introduced security concerns for classical channels, due to their potential to undermine classical cryptographic approaches. This paper, therefore, considers the adoption of quantum-enabled learning with quantum communication protocol, especially quantum secure direct communication (QSDC) via superdense coding. While the processing learning happens across different locations for next-generation WIoE networks, the QSDC prevents vulnerabilities of data poisoning and model stealing in connected quantum collaborative learning.**

I. Introduction

WIRELESS INTERNET-of-Everything (WIoE) is an extension of Internet-of-Things (IoT) for the sixth-generation wireless communication (6G) and beyond application. Sensors generate an increasing influx of data to enable interaction between people and everything, such as real and virtual environments. Integrating artificial intelligence (AI) across all layers of beyond 6G networks, such as machine learning (ML) for resource allocations [1] and interference management [2] in wireless communications, is essential for extensive computational data in the WIoE, as it excels in interpreting information and recognizing data patterns. Nevertheless, it grows increasingly complex as it evolves into dense, heterogeneous ecosystems with massive device connectives. Optimizing such cross-domain systems poses major scalability concerns, demanding intelligent, adaptive learning workflows [3], [4]. Compounding the issue, the miniaturization of classical transistors has already reached its physical limits, signaling the need for alternative computing technologies to meet future demands.

Quantum technology has been widely investigated by engineers, not only for the field of physics but, notably, for its utilization in computations and communications. The current noisy intermediate-scale quantum (NISQ) computers already show potential to outperform classical computers for specific essential tasks, as shown in [5] and [6], among other instances. Furthermore, quantum-enabled learning has garnered substantial interest ranging from future wireless networks [7], directing unmanned aerial vehicle (UAV) trajectory [8], to tactical augmented reality [9]. Still, tangible risks are inherent in centralized quantum-enabled learning, wherein the central unit performs the entirety of the computational heavy lifting, rendering the central unit a single point of failure and scalability. These concerns prompt the advancement of non-centralized quantum-enabled learning, which we termed quantum collaborative learning (QCL), in the form of quantum federated learning, ensemble learning, and other such workflows.

To address this, leading studies have promoted that quantum communication protocol is a secure communication using the principles of quantum mechanics, where protocols utilize entangled qubits to communicate between quantum processing nodes that exposing any attempt to eavesdrop on one, and forbidding perfect copying of quantum state, which is known as the no-clone theorem. Capitalizing on these benefits, this study introduces quantum connected collaborative learning (QCCL), utilizing a superdense coding protocol [10] to connect different learning models, as illustrated in Fig. 1. As a proof-of-concept, this study leverages QCCL to maximize clients' achievable sum rate in WIoE, given their varying channel conditions. This paper directly confronts the contributions through the following key points: (i) While prominent studies do employ distributed learning models in collaborations, as in robust quantum federated learning, e.g., [11] and multi-agent quantum deep reinforcement learning, e.g., [12], quantum communication protocols are unfortunately left unutilized in these studies. This paper, therefore, introduces the notion of QCCL, in which different quantum learning models are integrated with quantum communications. (ii) This paper provides workflow designs for adopting quantum secure direct communications. This approach not only directly addresses the security concerns of quantum collaborative learning but also opens possibilities that are unthinkable without it. Specifically,

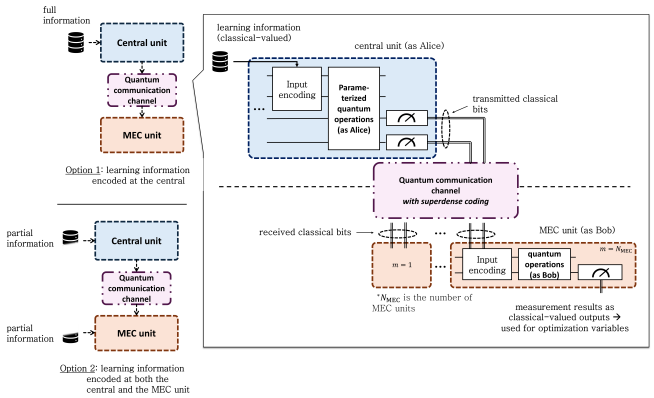

Fig. 1: An overview of the proposed QCCL involving a central and multi-access edge computing (MEC) unit, leveraging quantum communications for information exchange.

it adopts a design guide that can be extended to other communication protocols and models, making this paper distinctive, providing such a guide for quantum communication-enabled learning interconnections.[1] (iii) This study demonstrates the utility of QCCL to optimize wireless networks, particularly for supporting WIoE, considering a practical objective to optimize a small transceiver's parameters, aiming to maximize the sum rates of clients. At the time of writing, this is an earlier study that considers the utility of collaborative learning, let alone superdense encoding employments.[2]

II. WIoE Model

We study a WIoE network where a small access point (AP), equipped only with a single antenna, serves K_{user} single-antenna clients in wireless downlink communications. We use an MEC unit capable of quantum computing and communication that connects with AP. The MEC and a central unit are in different locations and connected via a quantum channel, sharing entangled qubits to facilitate quantum communications. Nevertheless, as per WIoE directives, this MEC has limited memory capacity and must therefore send learning datasets directly to the central unit for processing via quantum computing. At each iteration time t, given N_{sub} frequency allocations, the wireless channel between the AP and the clients, a key factor influencing the network's performance, can be expressed as $\mathbf{h}^{(t)} = [\{h_{m,k}^{(t)}\}_{k=1}^{K_{\text{user},m}}]_{m=1}^{N_{\text{sub}}} \in \mathbb{C}^{1\times K_{\text{user}}}$, where $K_{\text{user},m}$ denotes the number of users occupying the m-th frequency allocation, and $h_{m,k}^{(t)}$ denotes the channel coefficient of the (m,k)-th client among them, and where $K_{\text{user}} = \sum_{m=1}^{N_{\text{sub}}} K_{\text{user},m}$.

Given the aforementioned minimal transmit equipment and limited transmit power typical in WIoE networks, the small AP is expected to maximize the sum rate of the clients while satisfying the quality-of-service (QoS) of each k-th client, as defined in the following:

$$\underset{\mathbf{p}_{\text{Tx},k}^{(t)}}{\text{maximize}} \quad \sum_{m=1}^{N_{\text{sub}}} \sum_{k=1}^{K_{\text{user},m}} \mathsf{R}_{m,k}^{(t)} \tag{1a}$$

$$\text{subject to} \quad \mathsf{R}_{k}^{(t)} \geq \mathsf{R}_{\text{min}}, \tag{1b}$$

$$p_{\text{Tx},k}^{(t)} \leq \hat{P}_{\text{Tx}}, \tag{1c}$$

where $\mathbf{p}_{\text{Tx}}^{(t)} = \left[\left\{p_{\text{Tx},m,k}^{(t)}\right\}_{k=1}^{K_{\text{user},m}}\right]_{m=1}^{N_{\text{sub}}} \in \mathbb{C}^{1\times K_{\text{user}}}$ denotes the vector of transmit power allocations, by which $p_{\text{Tx},m,k}^{(t)}$ is associated with the k-th user occupying the m-th sub-band. The constraint in (1b) enforces a minimum allowed rate R_{min} as it may need to send multimedia content in addition to the requirement for sensors only. The constraint in (1c) deals with the transmit power budget, accounting for compliance with the maximum transmit power $\hat{P}_{\text{Tx}}$. To adhere to it, we optimize the power coefficients for each t, where $e_k^{(t)}$ denotes the normalized coefficient for the k-th user, abiding by $e_1^{(t)} + \cdots + e_k^{(t)} + \cdots + e_K^{(t)} = 1$. The allocated power for each k-th user is then given by $p_{\text{Tx},k} = e_k^{(t)} \hat{P}_{\text{Tx}}$, $\forall k$.

The rate of each k-th user depends on several factors, including the multiple access technique used, prominent examples including partial non-orthogonal multiple access (pNOMA) and power-domain non-orthogonal multiple access (PD-NOMA) [18]. These two techniques pair certain clients and then assign distinct transmit power to each according to their channel gains. To streamline the analysis, we arrange the clients' indices according to their channel gains: $|h_{m,1}^{(t)}|^2 > \cdots > |h_{m,K_m}^{(t)}|^2$, where K_m marks the number of clients within the m-th pair. When we employ pNOMA in particular, the achievable rate of the l-th client, with the use of the m-th sub-band b_m, is given by:

$$R_{m,l} = b_m \log_2\left(1 + \frac{|h_{m,l}^{(t)}|^2 \; p_{\text{Tx},m,l}^{(t)}}{\sigma_{m,l}^{(t)} + \sum_{i=1}^{l-1} |h_{m,l}^{(t)}|^2 \; p_{\text{Tx},m,i}^{(t)}}\right), \tag{2}$$

where the denominator of the signal-to-noise ratio accounts for inter-pair interferences.

III. Proposed Scheme

To optimize WIoE, we use QCCL that integrates distributed learning with quantum communication and computation, as depicted in Fig. 1.[3] We assume a vastly more capable central processing unit, one that commands a large count of logical qubits. It further assumes the responsibility for mapping the classical-valued learning information, represented by $\mathbf{X}_{\text{cent}}^{(t)}$, into Hilbert spaces, via a particular unitary $\mathsf{U}_{\text{cent,A}}(\mathbf{X}_{\text{cent}}^{(t)})$, to be computed through its quantum circuit. In adjusting the output of the learning model, parameterized quantum operations are subsequently used, illustrated by the unitary $\mathsf{U}_{\text{cent,B}}(\mathbf{w}_{\text{cent}}^{(t)})$, with $\mathbf{w}_{\text{cent}}^{(t)}$ denoting its parameters. The resulting outputs are

[1] By comparison, pertinent studies either lean toward providing workflows to support the execution of quantum algorithms, e.g., such as [13], addressing hardware and computations, e.g., [14], or focusing on quantum communication protocols [15].

[2] For example, the pertinent study in [16] employ an evolutionary algorithm-based approach, while [17] considers classical reinforcement learning.

[3] We focus on option 1 throughout this paper, as it is more likely to be implemented in the near future, given the limited quantum computing capabilities on MECs.

in classical bits, obtained via quantum measurements and expressed as the vector $\mathbf{c}_{\text{cent}}^{(t)} = \left[c_{\text{cent},j}^{(t)}\right]_{j=1}^{N_{\text{bits}}} \in \{0,1\}^{1\times N_{\text{bits}}}$, where $c_{\text{cent},j}^{(t)}$ is the j-th individual bit of the N_{bits}-length classical bits These bits are transmitted to the MEC unit via a quantum communication protocol, particularly superdense coding, which impressively conveys two bits of information per an entangled qubit. Upon receiving the qubit, the MEC then measures the pair of entangled qubits to decode the designated information as classical bits. At time t, these bits can be denoted as the vector $\mathbf{c}_{\text{MEC}}^{(t)} = \left[c_{\text{MEC},i}^{(t)}\right]_{i=1}^{N_{\text{bits}}} \in \{0,1\}^{1\times N_{\text{bits}}}$, in which $c_{\text{MEC},i}^{(t)}$ signifies the i-th bit: an ideal, lossless channel shall allow $\mathbf{c}_{\text{MEC}}^{(t)} = \mathbf{c}_{\text{cent}}^{(t)}$. Subsequently, these bits are used to control pertinent quantum operations, as the unitary $\mathsf{U}_{\text{MEC,A}}(\mathbf{c}_{\text{MEC}}^{(t)})$, followed by an entanglement operation, $\mathsf{U}_{\text{MEC,B}}$.

As illustrated in Fig. 1, we employ a quantum communication protocol, superdense coding [10], to communicate between the central processing unit and the MEC, leveraging its inherent communication efficiency and reliable security. To illustrate its working principle, let us consider a transmitted bit vector $\left[c_{\text{cent},j}^{(t)}\right]_{j=1}^{N_{\text{bits}}}$ with $N_{\text{bits}} = 2$. Initially, a pair of entangled qubits is prepared for both the central unit and the MEC, in the Bell state $|\Phi^+\rangle = \mathsf{C}_x(0,1)\cdot(\mathsf{H}_0\otimes\mathbb{I}_1)\cdot|0\rangle^{\otimes 2}$. Leveraging the superdense coding protocol, the central unit encodes its share of the entangled qubit pair, according to $\mathbf{c}_{\text{cent},j}^{(t)}$. The bit pair in $\mathbf{c}_{\text{cent},j}^{(t)}$ dictates the quantum gate applied in the encoding part of the superdense coding protocol, resulting in four distinguishable quantum states: if $\mathbf{c}_{\text{cent},j}^{(t)} = \{0,0\}$, $\{0,1\}$, $\{1,0\}$, or $\{1,1\}$, then we apply I_0, X_0, Z_0, and X_0 Z_0, respectively, X_0 and Z_0 denote the application of the Pauli-X and -Z gates onto the central unit's qubit, respectively. Once encoded, this qubit is then sent through the quantum channel to the MEC, with the entangled Bell state facilitating secure information transfer.

On the MEC side, to recover the classical information sent by the central unit, Bell state measurement is performed. This involves applying the unitary operation $(\mathsf{H}_0\otimes\mathbb{I}_1)\cdot\mathsf{C}_x(0,1)$ to the pair of entangled qubits (MEC's own qubit and the received qubit from the central unit), followed by measurement in the computational basis, yielding classical bits.[4] As such, this process allows two classical bits to be transmitted by sending a single qubit. To accommodate larger messages, we generalize this approach to support the transmission of $N_{\text{bits}} = 2N$ classical bits, where N is the number of shared entangled qubit pairs, as illustrated in Fig. 2. The process of quantum communication similarly begins with the preparation of the entangled qubit pairs. To generalize for larger-scale communication, we distinguish the central unit's

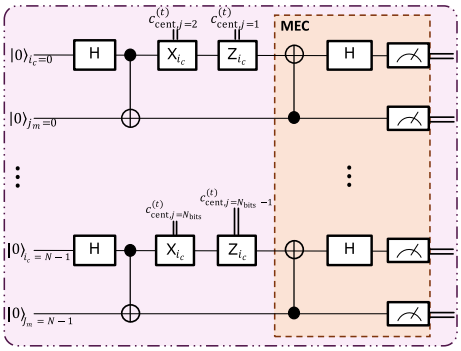

Fig. 2: Quantum communication circuit with superdense enabling transmission of multiple classical bits from the central unit to the MEC.

qubits and those of the MEC, by indexing them as $i_c \in \{0,\ldots,N-1\}$ and $j_m \in \{0,\ldots,N-1\}$, respectively. Qubits with matching indices are paired together, e.g., $i_c = 2$ and $j_m = 2$. Thereby, the state of the entangled qubit pairs can be prepared as: $|\psi_{\text{QC,A}}\rangle = \mathsf{U}_{\mathsf{initSDC}}\cdot\left\{\bigotimes_{i_c,j_m=0}^{N-1}(|0\rangle_{i_c}\otimes|0\rangle_{j_m})\right\}$, where $\mathsf{U}_{\mathsf{initSDC}} = \bigotimes_{i_c=0}^{N-1}\mathsf{C}_x(i_c, j_m = i_c)\cdot[\mathsf{H}_{i_c}\otimes\mathbb{I}_{j_m=i_c}]$ is the initialization operator. The values of $2N$ classical bits are then encoded to the states of N qubits, using a combination of Pauli X and Z gates, as follows: $\mathsf{U}_{\text{QC,enc}} = \bigotimes_{i_c=0}^{N-1}\left((X_{i_c})^{c_{\text{cent},j=2(i_c+1)}^{(t)}}\cdot(Z_{i_c})^{c_{\text{cent},j=2(i_c+1)-1}^{(t)}}\right)\otimes\mathbb{I}_{j_m=i_c}$.[5] Upon receiving the transmitted qubits, the MEC performs Bell state measurement defined by $\mathsf{U}_{\text{QC,B}} = \bigotimes_{i_c=0}^{N-1}[\mathsf{H}_{i_c}\otimes\mathbb{I}_{j_m=i_c}]\cdot\mathsf{C}_x(i_c, j_m = i_c)$, recovering the $2N$ classical bits encoded earlier. Eventually, the full state evolution of the transmitted qubits is given by

$$|\psi_{\text{QC}}\rangle = \mathsf{U}_{\text{QC,B}}\cdot\mathsf{U}_{\text{QC,enc}}\cdot|\psi_{\text{QC,A}}\rangle\,. \tag{3}$$

Upon executing measurement on $|\psi_{\text{QC}}\rangle$, the quantum system collapse unto a computational basis state $\left\{|\text{bin}(i)\rangle \;\middle|\; i\in\{0,1,\ldots,2^N-1\}\right\}$, representing the original classical information sent from the central unit to the MEC.[6]

Regarding the MEC unit's learning model, the first operation encodes the classical bits received and is given by: $\mathsf{U}_{\text{MEC,A}} = \sum_{m=1}^{N_{\text{sub}}}\left(\mathsf{R}_y\left(\tanh(c_{\text{MEC},m,\text{a}}^{(t)})\pi\right)\otimes\mathsf{R}_y\left(\tanh(c_{\text{MEC},m,\text{b}}^{(t)})\pi\right)\right)$, where $c_{\text{MEC},m,\text{a}}^{(t)}$ and $c_{\text{MEC},m,\text{b}}^{(t)}$ are among the received classical bits by MEC. Each binary representation can either be interpreted directly or linearly mapped to a corresponding level within a continuous range, e.g., $0 \to 0.25$ and $1 \to 0.75$, depending on the chosen quantization strategy. Such quantization approaches are common to represent continuous-valued wireless communication parameters, such as transmit power allocation, using classical bits. For instance, representing φ transmit power allocation levels requires $\lceil\log_2(\varphi)\rceil$ classical bits. Nonetheless, thanks to the superdense coding protocol, every two of these bits can be

[4] A Bell state measurement projects a pair of qubits into one of four Bell states, which are identified through corresponding outcomes in the computational basis. For instance, the Bell state $|\Phi^-\rangle = \frac{1}{\sqrt{2}}(|00\rangle - |11\rangle)$ is mapped to the computational basis $|10\rangle$.

[5] For instance, $(X_{i_c})^{(1)}$ or $(X_{i_c})^{(0)}$ indicate that we apply or omit the Pauli X operation on the qubit i_c, respectively.

[6] $\text{bin}(i)$ denotes the binary representation of the integer i as a bit string, e.g., from $\text{bin}(4) = 100$.

transmitted by the cloud unit via a single qubit, provided that it shares an entangled qubit pair with the MEC unit. The second operation connects different qubits operated by the MEC unit, and is given as $\mathsf{U}_{\text{MEC,B}} = \sum_{m=1}^{N_{\text{sub}}-1} \mathsf{C}_z$. The learning model processed by the MEC unit can be expressed as $\mathsf{U}_{\text{MEC}} = \mathsf{U}_{\text{MEC,B}}\mathsf{U}_{\text{MEC,A}} |\psi_{\text{MEC}}^{\text{init}}\rangle$, in which the initialized state is typically prepared as $|\psi_{\text{MEC}}^{\text{init}}\rangle = |0\rangle^{\otimes 2N_{\text{sub}}}$. While there are viable opportunities to use parameterized operations for the MEC unit's model, we henceforth focus on entangled operations, to simplify the learning processes, and to delegate them to the central unit, which is expected to surpass the MEC unit in capability.

The central unit's learning model can be deconstructed as follows. Upon first leveraging the encoding operation $\mathsf{U}_{\text{cent,A}}$, the following operation comprising L layers is executed, as provided here:

$$\mathsf{U}_{\text{cent,B}} = \Bigg[\prod_{l=1}^{L} \Big\{ \mathsf{C}_x(|\psi_{N_{\text{qubit}}^{(l)}}\rangle, |\psi_0\rangle) \Big(\prod_{i=1}^{N_{\text{qubit}}^{(l)}} \mathsf{C}_x(|\psi_i\rangle, |\psi_{i+1}\rangle) \Big) \bigotimes_{i=1}^{N_{\text{qubit}}^{(l)}} \mathsf{R}_y\left(\tanh(w_{l,i})\right) \Big\} \Bigg], \tag{4}$$

where $N_{\text{qubit}}^{(l)}$ signifies the number of qubits involved in the l-th layer. The learning model of the central unit can then be expressed as $|\psi_{\text{cent}}\rangle = \mathsf{U}_{\text{cent,B}}\mathsf{U}_{\text{cent,A}} |\psi_{\text{cent}}^{\text{init}}\rangle$, where the qubits are prepared as $|\psi_{\text{cent}}^{\text{init}}\rangle = (\mathsf{H}|0\rangle)^{\otimes n}$, and $\mathsf{U}_{\text{cent,A}} = \Big(\bigotimes_{i=1}^{N_{\text{qubit}}^{(l)}} \mathsf{R}_{\text{y}}\big(\tanh(\text{Re}(x_i))\pi\big) \cdot \mathsf{R}_{\text{z}}\big(\tanh(\text{Im}(x_i))\pi\big) \Big)$. Again, there are vast possibilities of leveraging distinct quantum variational operations, much like employing various encoding approaches. To obtain the optimization variables in (1a), we use the measurement outcomes from the MEC's quantum model.[7]

IV. Performance Analysis

In this section, we evaluate the proposed QCCL within the context of optimizing a WIoE network. We consider two scenarios to evaluate our approach: grant-free and pNOMA (see Section II). Both share the same objective functions, i.e., maximizing the users' sum rate, as in Eq. (2). We performed the learning with information encoded at the central unit, Option 1, to maximize (2). In the classical setup, we set $\hat{P}_{\text{Tx}} = 10$ W, $K_{\text{user}} = 4$, $B = 5$ MHz, $\mathsf{R}_{\text{min}} = (1 \text{ bps/Hz} \cdot B)/K_{\text{user}} = 1.25$ Mbps, $N_{\text{eps}} = 50$, and $\mathbf{h}$ represents Rayleigh fading channel. We encoded the channel coefficients as input to a parameterized quantum circuit. We apply the parameter shift rule to compute the loss gradient, with $N_{\text{shots}} = 1024$. Simulations were performed using the IBM Qiskit-Aer platform simulator, assuming quantum communications under both perfect and imperfect conditions. When accounting for quantum communication imperfections, we consider the bit-flip error,

[7]The measurement results are directly used for optimization in our model and converted into normalized transmit power allocation coefficients, as $e_n \leftarrow \langle M_{\text{MEC},n} \rangle$, where $M_{\text{MEC},n} = |1\rangle\langle 1|$ is the observable measured on the MEC's n-th qubit.

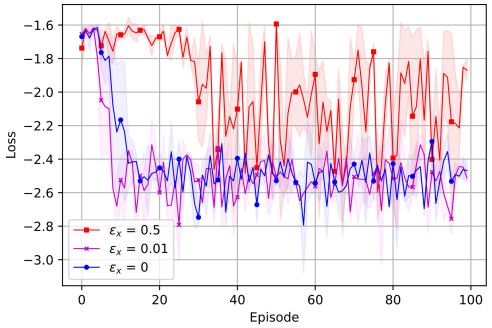

Fig. 3: QCCL training loss values under perfect and imperfect quantum communication, assuming grant-free access for all users.

whose effect is akin to Pauli-X gates with probability ε_x, thus modeled as a property of the following quantum channel $\mathcal{Q}$, presented through Kraus operators acting on the transmitted qubit ϱ. $\mathcal{Q} : \varrho = \mathsf{K}_0\varrho\mathsf{K}_0^{\mathsf{H}} + \mathsf{K}_1\varrho\mathsf{K}_1^{\mathsf{H}}$, where $\mathsf{K}_0 = \sqrt{\varepsilon_x - 1}\,\mathbb{I}$, and $\mathsf{K}_1 = \sqrt{\varepsilon_x}\,\mathsf{X}$. To update the circuit parameters, we calculate a training loss involving the objective function (i.e., sum-rate calculation) and a penalty term (for constraint violations), expressed as:

$$\mathcal{L} = -\mu_a \sum_{k}^{N_{\text{user}}} \mathsf{R}_k + \mu_b \sum_{k=1}^{N_{\text{user}}} \max(0, \mathsf{R}_{\text{min}} - \mathsf{R}_k), \tag{5}$$

where μ_a and μ_b are the weight factors associated with sum-rate maximization and constraint compliance, respectively. We set $\mu_a = 0.9$, where $\mu_a + \mu_b = 1$. As such, a larger μ_b prioritizes fairness while a smaller μ_b favors sum-rate maximization.

We train the superdense coding-connected collaborative learning architecture in Fig. 1, aiming to maximize the client sum-rate elaborated in Section II. Figure 3 compares QCCL performance under different quantum communication conditions, with $\epsilon_x = 0.5$ reflecting the worst case. As expected, $\epsilon_x = 0.5$ leads to significant loss fluctuations, while the other cases show clear learning progression during the first 20 episodes and then stabilize. We also extend the WIoE system model from grant-free to pNOMA to assess whether QCCL is applicable to different multiple access techniques and able to minimize the sum-rate loss calculation $\mathcal{L}$. We investigated its loss performance under perfect quantum channel conditions in Fig. 4, using three different quantization levels to show the impact of a higher level φ.[8] The proposed QCCL follows the unsupervised learning paradigm, towards maximizing the achievable sum rate, so that it does not require labeling in the loss functions, as in Eq. (2). This aligns well with real wireless applications, where the problem involves unlabeled data. Figure 5 shows a sum-rate comparison, between QCCL applied to pNOMA and grant-free scenarios, assuming $\epsilon_x = 0.1$. The proposed QCCL approach demonstrates improved training performance under imperfect quantum channels. The choice of multiple access techniques particularly affects the WIoE

[8]Since the optimization variables are heavily affected by the quantization of input values of the MEC unit, a higher quantization level φ resulted in a finer control over the power resource allocation coefficients.

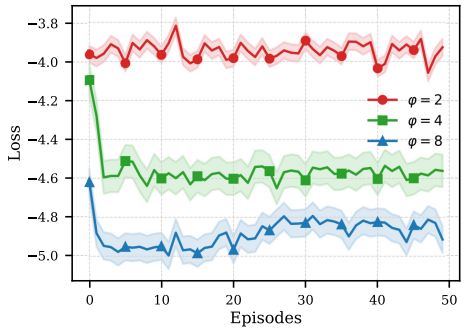

Fig. 4: The QCCL training loss values in the pNOMA scenario (see (2)) with different quantization levels φ.

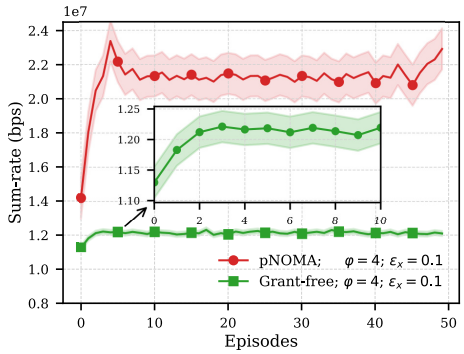

Fig. 5: The achieved sum-rate of QCCL in both grant-free and pNOMA scenarios, accounting for imperfections in quantum communication.

network performance, with pNOMA significantly outperforms the grant-free system model.

In the following, we investigate QCCL security, involving a central unit as a sender, an MEC unit as a receiver, and a single attacker (analogous to the archetypes "Alice," "Bob," and "Eve" in typical security analyses). Suppose the attacker, Eve, has the following objectives. First, the attacker intercepts the traveling qubit from Alice to Bob after encoding two classical bits. Nonetheless, Eve can not learn from the qubit since it is always in maximally mixed state $\frac{1}{2}I$, and Eve will break the entanglement of Alice and Bob, prompting the detection of the attack on test rounds; furthermore, the attacker also will not be able to copy of the quantum state, thanks to the no-cloning theorem. Second, the attacker may attempt to relay fabricated information to the MEC unit through its qubit, $|\psi_{\text{Eve}}\rangle$, which is not entangled with the central unit's qubits. As a result, Bob is likely to detect this statistically, observing Bell-state fidelity or correlations, as the measurement outcome will deviate from the expected measurement of the Bell state.

We evaluate the complexity of the proposed QCCL method by examining the number of gates and the total number of parameter operations within the quantum circuit. The proposed method comprises three segments: the parameterized quantum operations processed by the central units, the quantum operations processed by the MEC unit, and the quantum communication protocol to connect those two segments. Both the central and MEC units each leverage input encoding operations, respectively defined as $\mathsf{U}_{\text{cent,A}}$ and $\mathsf{U}_{\text{MEC,A}}$. The number of quantum gates requisite for each operations scales with the count of the transmitted classical bits: $\kappa\Big(\mathsf{U}_{\text{cent,A}}\big(\mathbf{X}_{\text{cent}}^{(t)}\big)\Big) = 2N_{\text{bits}}$ and $\kappa\Big(\mathsf{U}_{\text{MEC,A}}\big(\mathbf{c}_{\text{cent}}^{(t)}\big)\Big) = N_{\text{bits}}$, where the function $\kappa(\cdot)$ denoting the number of quantum gates. As an example, we consider $N_{\text{bits}} = 4$. Accordingly, the total number of gates required for $\mathsf{U}_{\text{cent,B}}$ and $\mathsf{U}_{\text{MEC,B}}$ are given by $\kappa(\mathsf{U}_{\text{cent,B}}) = 2N_{\text{bits}} = 8$ and $\kappa(\mathsf{U}_{\text{MEC,B}}) = N_{\text{bits}} - 1 = 3$, respectively. The number of gates for a quantum communication channel depends on the classical bits output from the central unit, as we use the superdense coding operation $\mathsf{U}_{\text{QC,enc}}$ that uses Z and/or X gates. Both $\mathsf{U}_{\text{QC,A}}$ and $\mathsf{U}_{\text{QC,B}}$ therefore require the same number of gates, given by $\kappa(\mathsf{U}_{\text{QC,A}}) = \kappa(\mathsf{U}_{\text{QC,B}}) = N_{\text{bits}}$. Therefore, for $N_{\text{bits}} = 4$, the whole quantum system requires $\kappa\Big(\mathsf{U}_{\text{cent,A}}\Big) + \kappa\Big(\mathsf{U}_{\text{cent,B}}\Big) + \kappa\Big(\mathsf{U}_{\text{MEC,A}}\Big) + \kappa\Big(\mathsf{U}_{\text{MEC,B}}\Big) + \kappa\Big(\mathsf{U}_{\text{QC}}\Big) = 7N_{\text{bits}}$ gates.[9]

We also evaluated the entanglement capability of the entire QCCL operation using the Meyer-Wallach (MW) measure. In addition, an ideal distributed quantum-enabled learning scenario is also presented for comparison, in which the decoding result from the cloud unit, $\langle M_{\text{cent}}\rangle$, is directly transmitted to the MEC unit. The general MW measure on a quantum state $|\psi\rangle$, given N_{qubits} qubits, can be written as $Q(|\psi\rangle) = \frac{4}{N_{\text{qubits}}}\sum_{j=1}^{N_{\text{qubits}}} D\big(\iota_j(0)|\psi\rangle, \iota_j(1)|\psi\rangle\big)$, where $D(\mathbf{u},\mathbf{v}) = \sum_{i,j}|u_i v_j - u_j v_i|^2$ represents the squared area of the parallelogram spanned by vectors $\mathbf{u}$ and $\mathbf{v}$, and where $\iota_j(b)|\psi\rangle$ is a linear map acting similarly to a Kronecker delta filter, projecting $|\psi\rangle$ into a reduced Hilbert space $\mathbb{C}^{2^{N_{\text{qubits}}-1}}$. The linear map can be written as $\iota_j(b)|\psi\rangle = \delta_{b,b_j}|b_1\ldots,\hat{b_j},\ldots,b_N\rangle$, where $b \in \{0,1\}$ and $\hat{b}_j$ is the omission of the j-th bit.

The parameterized circuits within QCCL evolve as functions of their trainable parameters. To quantify their overall entangling capability, we compute the average MW measure over a set of parameters sampled uniformly from $[0, 2\pi)$, while keeping the classical-valued learning information fixed: $\langle Q\rangle = \frac{1}{|\mathbf{s}|}\sum_{\theta_i\in\mathbf{s}} Q(|\psi_{\theta_i}\rangle)$, where $\mathbf{s} = \{\theta_i\}$, $\theta_i \sim \mathcal{U}(0, 2\pi)$, and where $|\psi_{\theta_i}\rangle$ indicates the output state of the parametrized circuit for the given parameter θ_i. Table I shows that while QCCL retains significant entangling capacity, it falls slightly short of the ideal information transfer scenario, in which information is transmitted without quantization or noise. This indicates a trade-off introduced by leveraging superdense coding to partition the learning model into sub-models. Our analysis attributes this reduction primarily to the quantization process required to map the transmitted qubit onto optimization variables. In light of this, Fig. 6 compares the performance

[9]The total number of trainable parameters is typically tied to the learning process. As such, the quantum communication protocol lacks such parameters, only the circuits of the central and MEC units are involved in learning. Each employs $\mathsf{U}_{\text{cent,B}}$ and $\mathsf{U}_{\text{cent,A}}$ for the parameterized quantum circuit, both having the same number of parameters, as indicated by $\vartheta(\text{cent}) = \vartheta(\text{MEC}) = N_{\text{bits}}$. The whole QCCL workflow, therefore, has a total of $\vartheta_{\text{total}} = \vartheta(\text{cent}) + \vartheta(\text{MEC}) = 2N_{\text{bits}}$ parameters.

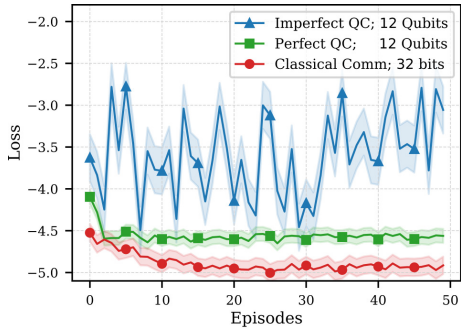

Fig. 6: The QCCL training loss value in the pNOMA scenario with different setups.

TABLE I: Comparison of MW entanglement capability and the average loss of using QCCL in three different setups.

Setup	Description	$\langle Q \rangle$	Avg. Loss Grant-Free	Avg. Loss p-NOMA
QCCL	cent $\rightarrow$ QC $\rightarrow$ MEC (Quantization)	0.439	-2.427	-4.561
QCCL with noise	cent $\rightarrow$ QC ($\varepsilon_x = 0.5$) $\rightarrow$ MEC (Quantization)	0.207	-1.945	-3.595
Ideal	cent $\rightarrow$ MEC	0.476	-2.499	-4.886

of QCCL with that of classical communication connecting the cloud and MEC, in the pNOMA scenario. The numbers of qubits and bits in Fig. 6 represent the required communication resources, whether quantum or classical communication is used. While classical communication performs better in average by about $\sim 7.13\%$ compared to QSDC under perfect channel conditions, the number of classical bits required in the classical communication case is more than double that of QCCL.[10]

V. Conclusion and Future Works

This study introduces QCCL, utilizing protocols such as superdense coding to connect different quantum learning models, facilitating optimizations over a wider geographic area, particularly in maximizing the achievable sum-rate in the WIoE networks. The proposed QCCL links the cloud's and the MEC's learning models, facilitating collaborative learning. We investigate its performance under noisy quantum channels, particularly under bit-flip error. It shows favorable performance despite the need to quantize the cloud's output before sending it over the quantum channel, as the superdense protocol transmits information in binary. Prospective developments include communication-efficient quantum collaborative learning, particularly through the quantization and sparsification of the transmitted information [19], and the use of multiple learning agents. In further advancing multi-agent learning, it is important to account for varying training levels of different learning models. Therefore, approaches based on imitation learning should be investigated in facilitating the learning of the less trained models, potentially via imperfect experts' demonstrations as well [20].

[10]Since traditional communication uses bits, continuous values must be converted into a bit sequence, e.q., we convert the continuous value c into the scaled range $[0, 255]$, which requires 8 bits. This is done by computing $\lceil c \cdot 255 \rceil$.

References

[1] D. G. S. Pivoto, F. A. P. de Figueiredo, C. Cavdar, G. R. d. L. Tejerina, and L. L. Mendes, "A comprehensive survey of machine learning applied to resource allocation in wireless communications," *IEEE Commun. Surv. Tutor.*, early access, Mar. 17, 2025, doi: 10.1109/COMST.2025.3552370.

[2] X. Liu, H. Zhang, K. Long, A. Nallanathan, and V. C. M. Leung, "Distributed unsupervised learning for interference management in integrated sensing and communication systems," *IEEE Trans. Wireless Commun.*, vol. 22, no. 12, pp. 9301–9312, Dec. 2023.

[3] H. Huang, J. Yang, H. Huang, Y. Song, and G. Gui, "Deep learning for super-resolution channel estimation and doa estimation based massive mimo system," *IEEE Trans. Veh. Technol.*, vol. 67, no. 9, pp. 8549–8560, Sep. 2018.

[4] M. Nerini, V. Rizzello, M. Joham, W. Utschick, and B. Clerckx, "Machine learning-based CSI feedback with variable length in FDD massive MIMO," *IEEE Trans. Wirel. Commun.*, vol. 22, no. 5, pp. 2886–2900, May 2023.

[5] A. D. King *et al.*, "Beyond-classical computation in quantum simulation," *Science*, vol. 388, no. 6743, pp. 199–204, Mar. 2025.

[6] Y. Kim *et al.*, "Evidence for the utility of quantum computing before fault tolerance," *Nature*, vol. 618, no. 7965, pp. 500–505, Jun. 2023.

[7] B. Narottama and T. Q. Duong, "Quantum neural networks for optimal resource allocation in cell-free mimo systems," in *Proc. IEEE Glob. Commun. Conf. (GLOBECOM)*, 2022, pp. 2444–2449.

[8] Silvirianti, B. Narottama, and S. Y. Shin, "UAV coverage path planning with quantum-based recurrent deep deterministic policy gradient," *IEEE Trans. Veh. Technol.*, vol. 73, no. 5, pp. 7424–7429, May. 2024.

[9] A. A. Okine, Silvirianti, and G. Kaddoum, "Quantum machine learning for multi-robot-assisted tactical augmented reality," *IEEE Internet Things Mag.*, vol. 8, no. 2, pp. 46–53, Mar. 2025.

[10] C. H. Bennett and S. J. Wiesner, "Communication via one- and two-particle operators on einstein-podolsky-rosen states," *Phys. Rev. Lett.*, vol. 69, pp. 2881–2884, Nov 1992.

[11] L. Chen, L. Yan, and S. Zhang, "Robust quantum federated learning with noise," *Phys. Scr.*, vol. 99, no. 7, p. 076003, Jun. 2024.

[12] R. Yan, Y. Wang, Y. Xu, and J. Dai, "A multiagent quantum deep reinforcement learning method for distributed frequency control of islanded microgrids," *IEEE Trans. Control Netw. Sys.*, vol. 9, no. 4, pp. 1622–1632, Dec. 2022.

[13] B. Weder, J. Barzen, M. Beisel, and F. Leymann, "Provenance-preserving analysis and rewrite of quantum workflows for hybrid quantum algorithms," *SN Comput. Sci.*, vol. 4, no. 3, p. 233, Feb. 2023.

[14] K.-C. Chen, X. Li, X. Xu, Y.-Y. Wang, and C.-Y. Liu, "Quantum-classical-quantum workflow in quantum-HPC middleware with GPU acceleration," in *Proc. 2024 Int. Conf. Quantum Commun., Netw., Comput.*, 2024, pp. 304–311.

[15] A. Dahlberg *et al.*, "A link layer protocol for quantum networks," in *Proc. ACM SIGCOMM Conf. Data Commun. (SIGCOMM)*, 2019, pp. 159–173.

[16] S. P. Singh, N. Kumar, A. Singh, K. Kant Singh, S. S. Askar, and M. Abouhawwash, "Energy efficient hybrid evolutionary algorithm for internet of everything (IoE)-enabled 6G," *IEEE Access*, vol. 12, pp. 63 839–63 852, Apr. 2024.

[17] P. Liu, K. An, J. Lei, Y. Sun, W. Liu, and S. Chatzinotas, "Computation rate maximization for SCMA-aided edge computing in IoT networks: A multi-agent reinforcement learning approach," *IEEE Trans. Wireless Commun.*, vol. 23, no. 8, pp. 10 414–10 429, Aug. 2024.

[18] H. Shakhatreh, S. Abdel-Razeq, and A. Al-Fuqaha, "Utilizing partial non-orthogonal multiple access (P-NOMA) in drone-enabled internet-of-things wireless networks," *IEEE Open J. Vehicular Technol.*, vol. 5, pp. 1088–1105, Aug. 2024.

[19] X. Cao *et al.*, "Communication-efficient distributed learning: An overview," *IEEE J. Sel. Areas Commun.*, vol. 41, no. 4, pp. 851–873, Apr. 2023.

[20] M. Zare, P. M. Kebria, A. Khosravi, and S. Nahavandi, "A survey of imitation learning: Algorithms, recent developments, and challenges," *IEEE Trans. Cybernetics*, vol. 54, no. 12, pp. 7173–7186, Dec. 2024.